

A Master Relation Defines the Nonlinear Viscoelasticity of Single Fibroblasts

Pablo Fernández, Pramod A. Pullarkat, and Albrecht Ott

Experimentalphysik I, Physikalisches Institut, Universität Bayreuth, D-95440 Bayreuth, Germany

ABSTRACT Cell mechanical functions such as locomotion, contraction, and division are controlled by the cytoskeleton, a dynamic biopolymer network whose mechanical properties remain poorly understood. We perform single-cell uniaxial stretching experiments on 3T3 fibroblasts. By superimposing small amplitude oscillations on a mechanically prestressed cell, we find a transition from linear viscoelastic behavior to power law stress stiffening. Data from different cells over several stress decades can be uniquely scaled to obtain a master relation between the viscoelastic moduli and the average force. Remarkably, this relation holds independently of deformation history, adhesion biochemistry, and intensity of active contraction. In particular, it is irrelevant whether force is actively generated by the cell or externally imposed by stretching. We propose that the master relation reflects the mechanical behavior of the force-bearing actin cytoskeleton, in agreement with stress stiffening known from semiflexible filament networks.

INTRODUCTION

Mechanical forces are essential for biological systems and their interaction with the environment. Tissues can generate forces, but forces also influence tissue development, as in embryogenesis, bone growth, or scar tissue formation (1). In vitro, single eukaryotic cells develop tension spontaneously on a substrate (2), and respond to extracellular elasticity (3). Cell mechanics is controlled by the cytoskeleton (4,5), a highly dynamic biopolymer network far from thermodynamic equilibrium. Its main components are actin, tubulin, and intermediate filaments. Different types of cross-linking proteins join these filaments into a myriad of geometries. Particularly interesting for cell mechanical properties are actin filaments, which can generate active forces through interaction with myosin motor proteins.

In the last years, much progress has been made in the study of reconstituted biopolymer systems with a known and limited number of components. The rheological behavior of such biopolymer networks has been experimentally studied and explained by simple models (6–10). Relating the so-gained framework to living cells, however, is a daunting task. Unlike passive networks, the actin cytoskeleton actively generates forces. Further, because of cytoskeleton restructuring or changes in motor activity, the mechanical behavior evolves in time. This evolution is controlled by signaling cascades, which in turn are influenced by mechanical perturbations.

Probing the mechanical properties of the actin network at the micrometer scale has become possible thanks to newly developed microrheological techniques (11–14). However, cell heterogeneity complicates the extrapolation of local

properties to the whole cell scale. Many-cell experiments, such as those on tissue or cell-populated gels (15–17), are efficient and reproducible, but they average over heterogeneous sets of cells interconnected by an extracellular matrix. This hampers an interpretation in single-cell terms. The quantitative study of the mechanical properties of entire, single cells is thus an essential step toward a global understanding of cell mechanics.

We report uniaxial stretching experiments on single 3T3 fibroblasts, suspended between two parallel, biochemically functionalized walls (see Fig. 1). This microplate rheometer allows us to clearly distinguish active behavior from the passive mechanical response to applied forces or strains (18).

MATERIALS AND METHODS

Experimental setup

We describe the main features of our cell rheometer, schematically shown in Fig. 2. This is an improved version of the original, home-built micromanipulation setup previously described (18). 3T3 Fibroblasts (19,20) are held between two parallel, coated glass microplates. One of them is rigid and provides a reference point. The other microplate is thin and narrow and therefore flexible, with an effective stiffness ~ 100 nN/ μ m, which is of the order of the elastic modulus of a typical fibroblast. Its bending provides the force acting on the cell in the y axis (see Fig. 2). The flexible microplate is translated by means of a piezoelectric actuator P-841.40 (Physik Instrumente, Karlsruhe, Germany) with a resolution of 1 nm. An optical fiber in contact with the flexible microplate couples microplate bending to translation of the emergent laser beam. The optical fiber is etched with hydrofluoric acid to a diameter of 6 μ m, so that its stiffness is far lower than that of the flexible plate and does not interfere with the force measurement. The cell is illuminated with green light and observed with an Axiovert 135 microscope (Zeiss, Oberkochen, Germany). A dichroic mirror separates the green illumination light from the He-Ne laser beam, which reaches an S-1880 two-dimensional position sensitive detector (Hamamatsu Photonics, Hamamatsu City, Japan) through one of the microscope ports. A personal computer reads the signal from the position detector, controls the piezoelectric actuator, and calculates the normal force F and the cell length ℓ . The precision in the

Submitted September 1, 2005, and accepted for publication January 17, 2006.

Address reprint requests to Pablo Fernández, Tel.: 49-921-55-2502; Fax: 49-921-55-2521; E-mail: pablo@ep1.uni-bayreuth.de.

© 2006 by the Biophysical Society

0006-3495/06/05/3796/10 \$2.00

doi: 10.1529/biophysj.105.072215

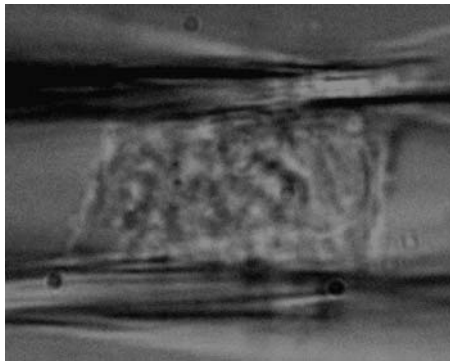


FIGURE 1 Image of an actively contracting fibroblast between two fibronectin coated microplates. The distance between plates is $\approx 5 \mu\text{m}$.

measurement of the fiber position is $\sim 100 \text{ nm}$. In most cases, a high resolution in time is not needed and averaging can improve the resolution to 30 nm . By controlling the piezoelectric translator, a feedback loop can impose user-defined force or length histories. The response time of the piezoelectric translator limits dynamic measurements to frequencies below 30 Hz . Due to the large length of the flexible microplate, its tip deflects by $< 6 \text{ arc min}$ during an experiment. Hence, the experimental geometry can be described as two parallel walls, which can be separated by a translation in the perpendicular direction.

Temperature control

The temperature of the cell-culture medium inside the chamber is controlled by means of two ITO-coated glass slides, one on the bottom of the chamber,

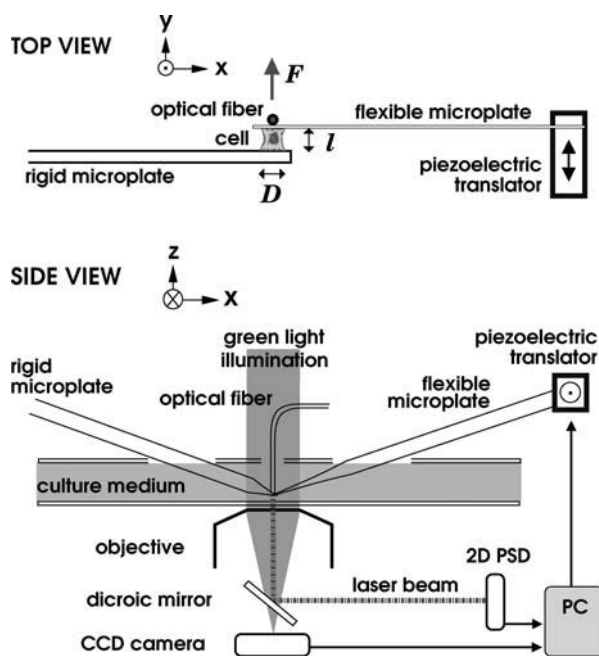


FIGURE 2 Schematic of the micromanipulation setup. A fibroblast is held between two coated microplates. The deformation of the flexible microplate gives the force F acting on the cell. The position of the laser beam emerging from the optical fiber, which is in contact with the tip of the flexible plate, is detected using a position sensitive detector. A personal computer reads the signal from the detector and controls the piezoelectric translator.

the other one above, with holes for the microplates and the optical fiber to pass through. To avoid convection in the medium, these slides are kept at different temperatures, imposing a temperature gradient pointing upward with a magnitude of $\sim 1^\circ\text{C}/\text{cm}$.

Microplates

The glass microplates used for the experiment are obtained by pulling glass strips (Vitrocom, Mountain Lakes, NJ) as described previously (18), using a modified P-97 Flaming/Brown micropipette puller (Sutter Instruments, Novato, CA). Microplates are then cleaned and coated with fibronectin from bovine plasma (Sigma-Aldrich, St. Louis, MO) or 3-aminopropyl triethoxysilane (Sigma-Aldrich) and glutaraldehyde (Fluka Chemie, Buchs, Switzerland).

Cell culture

Experiments where the cells stick to fibronectin-coated plates are performed in ISCOVE medium, with 25 mM HEPES buffer and 10% fetal bovine serum. Experiments with a glutaraldehyde coating start in pure saline solution to avoid inactivation of the coating by proteins and amino acids. After attachment of the cell to both plates, fetal bovine serum is added to a final concentration of 2% . All cell culture reagents are from Gibco (Invitrogen, Carlsbad, CA). 3T3 fibroblasts are obtained from the German Collection of Microorganisms and Cell Cultures (DSMZ, Braunschweig, Germany) (21).

RESULTS

Active response at constant cell length

We first perform experiments to characterize the response of fibroblasts to their presence in the rheometer (see Fig. 1). To stimulate contractility, we use high serum concentrations of 10% and fibronectin-mediated adhesion using coated microplates. Fibronectin binding to integrins is known to trigger the formation of focal complexes, which connect the extracellular matrix to the actin cytoskeleton (22,23). To minimize the mechanical perturbation to the cell, we keep constant the cell length ℓ , given by the distance between the rheometer microplates, and measure the force F . A typical response is shown in Fig. 3. After contact with the fibronectin coatings,

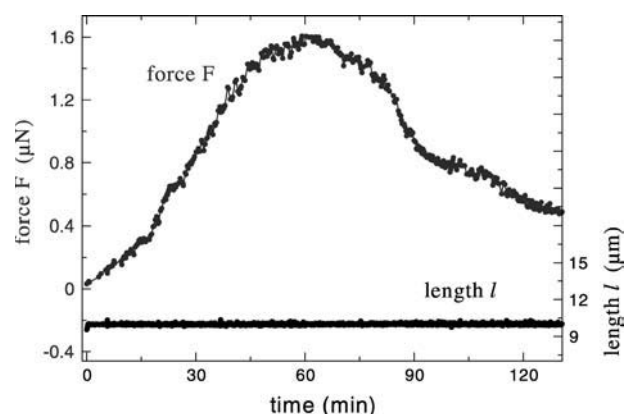


FIGURE 3 Force as a function of time at constant cell extension, recorded immediately after incorporation of the fibroblast into the rheometer. No significant cell shape alterations are seen throughout. The experiment is performed using fibronectin mediated adhesion.

most cells generate contractile tension, the force F reaches values up to $1 \mu\text{N}$, and eventually decays to zero. The force relaxation is an adaptation to the constant length condition, since active contraction can be induced again by a sudden change in cell length ℓ . The behavior is reproducible only in its broad, qualitative features. The force and timescales are strongly cell-dependent.

Dynamic viscoelastic moduli

To probe cell rheological properties during complex adaptive processes, we superimpose sinusoidal length oscillations at small amplitudes and high frequencies. These are chosen so that the corresponding maximum rate of change of force is at least two orders of magnitude above the values typically seen in active contraction.

Cells have both an elastic and a viscous response to imposed length oscillations (1,24). As the viscous response depends on deformation rate instead of absolute deformation, it causes a phase shift between length and force. The cell length is imposed as

$$\ell = \langle \ell \rangle + \Delta_\ell \sin(\omega t),$$

where $\langle \ell \rangle$ is the average length over an oscillation period, and Δ_ℓ is the amplitude of the superimposed length oscillations. In the linear regime, force is then given by

$$F = \langle F \rangle + \Delta'_F \sin(\omega t) + \Delta''_F \cos(\omega t).$$

We now introduce the initial contact area $A_0 = \pi (D/2)^2$, where D is the apparent cell diameter. The amplitudes are related by

$$\frac{\Delta'_F}{A_0} = \Theta' \frac{\Delta_\ell}{\langle \ell \rangle} \quad \text{and} \quad \frac{\Delta''_F}{A_0} = \Theta'' \frac{\Delta_\ell}{\langle \ell \rangle},$$

where Θ' and Θ'' are differential viscoelastic stretching moduli. The storage modulus Θ' reflects the purely elastic (nondissipative) part of the cell reaction, and the loss modulus Θ'' the viscous (dissipative) contribution. To compare cells of different sizes and with biological gels, we use formal engineering stress units for the moduli. Accordingly, stress is taken as $\sigma = F/A_0$.

The differential stretch moduli Θ' and Θ'' should not be confused with material parameters such as Young's modulus. The spatial distribution of force-bearing structure inside the cell is unknown. Rather than introducing ad hoc hypotheses, such as assuming a uniform material, we simply treat the cell as a mechanical black box. The unconventional symbol, Θ , for the moduli intends to emphasize their experiment-specific nature. Further, these moduli characterize the response of the material to small perturbations around a situation that may be far away from the resting state. Indeed, we show below that it is suitable to study Θ' and Θ'' as a function of the average force $\langle F \rangle$. A similar approach has been successfully used in stretching experiments on whole tissues, such as skin or muscle (1). Equivalent procedures

have recently been applied to biopolymer gels under shear deformations, where the differential shear moduli are measured as a function of the average stress or strain (6,7).

Instead of the loss and storage moduli Θ' and Θ'' , it will be more convenient to regard the absolute modulus $|\Theta|$ and the loss angle δ , defined as

$$|\Theta| = \sqrt{\Theta'^2 + \Theta''^2}$$

$$\delta = \arctan\left(\frac{\Theta''}{\Theta'}\right).$$

Fig. 4 shows the dependence of the stiffness $|\Theta|$ as a function of the strain amplitude $\Delta_\ell/\langle \ell \rangle$. In general, at strain amplitudes in the range 0.02–0.06, the moduli do not change by more than 20%. Moreover, no significant distortion of the response is seen below relative deformations of 0.1, as shown in Fig. 5. This holds irrespective of the frequency in the range 0.1–1 Hz. Thus, in subsequent experiments, the amplitude is kept small, $\Delta_\ell = 0.5 \mu\text{m}$, which corresponds for all cell length values to 0.02–0.06 strain amplitudes. More amplitude sweeps, including the amplitude dependence of the loss angle δ , can be found as Supplementary Material.

For completeness, in Fig. 6 we show preliminary results on the frequency dependence of the modulus $|\Theta|$ and the loss angle δ , in the range 0.1–1 Hz. We are currently modifying the setup to explore a wider frequency range, as at present we are limited to just one frequency decade. Keeping this in mind, our results are consistent with the literature on cell mechanics. On the average, $|\Theta|$ increases weakly with the frequency, whereas δ is approximately constant. The modulus $|\Theta|$ increases with the frequency roughly as a power law with exponents in the range 0.1–0.3. Such a frequency dependence, the signature of a flat, broad continuous spectrum

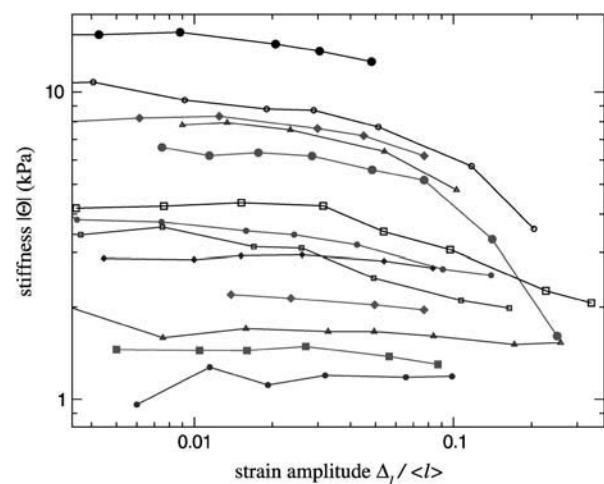


FIGURE 4 Amplitude sweep. Modulus $|\Theta|$ as a function of the strain amplitude $\Delta_\ell/\langle \ell \rangle$ for an arbitrary selection of cells, at a frequency of 0.2 Hz. Each curve is a different experiment; some at negative, compressive forces, some at positive tensions. No systematic change is seen in the shape of the amplitude sweeps as a function of force.

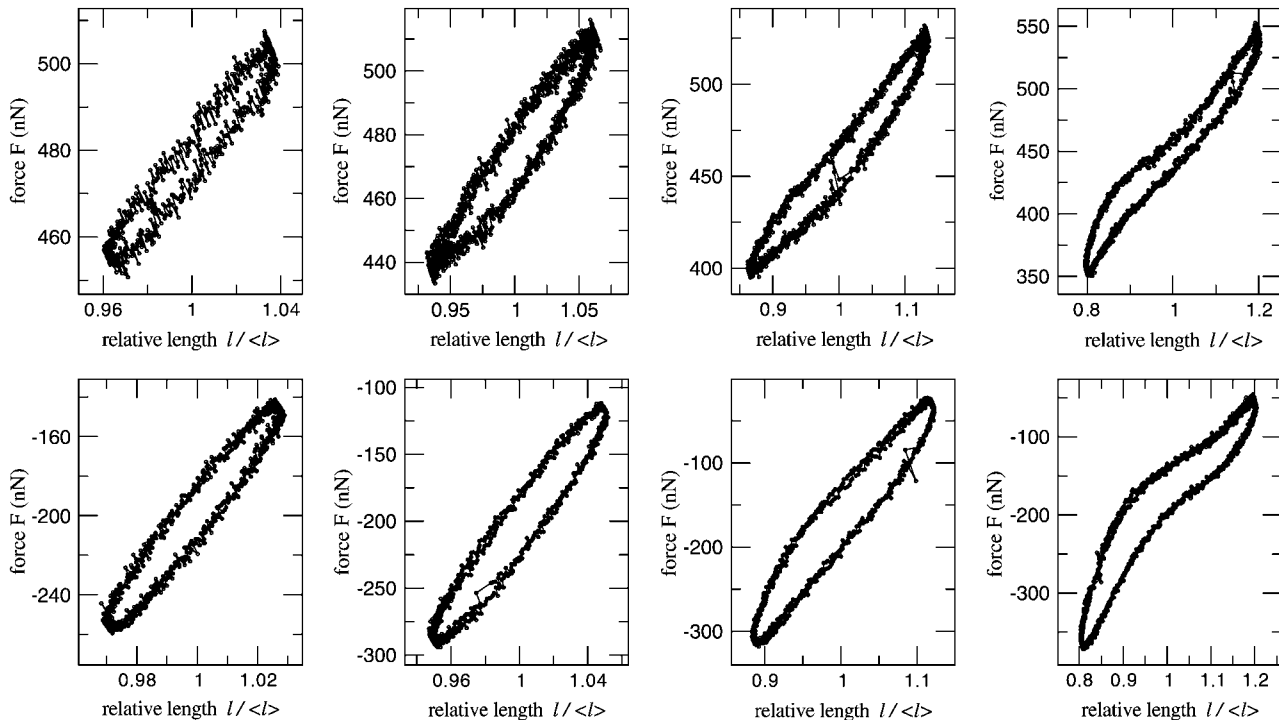


FIGURE 5 Lissajoux figures for different amplitudes. (Top) Typical response at forces above crossover. Force F as a function of relative cell length $\ell/\langle\ell\rangle$ for strain amplitudes 3.5%, 6%, 13%, and 20%. The oscillation frequency is 0.2 Hz. (Bottom) Typical response at compressive forces. Force F as a function of relative cell length $\ell/\langle\ell\rangle$ for strain amplitudes 3%, 5%, 12%, and 20%. The oscillation frequency is 0.2 Hz.

of relaxation times, has been known in soft tissues for a long time (1) and has recently been observed at the micrometer scale (14,25). Accordingly, recent experiments at the whole-cell scale performed with a setup similar to ours have revealed power law creep functions (26).

Stress stiffening at constant cell length

During the initial phase of force development after contact with the fibronectin-coated microplates, the cell sweeps force

space at a constant length. We superimpose sinusoidal oscillations to the constant average length to probe the temporal evolution of the moduli Θ' and Θ'' . The frequency of the oscillations is cyclically changed in the range 0.1–1.0 Hz. As shown in Fig. 7, as the average force increases with contractile activity of the cell, so does the modulus $|\Theta|$. Fig. 7 *c* and *d*, show the dependence of the response parameters $|\Theta|$ and δ on the average force $\langle F \rangle$ for different frequencies. This is an example of active stress stiffening, since it takes place at an average constant length.

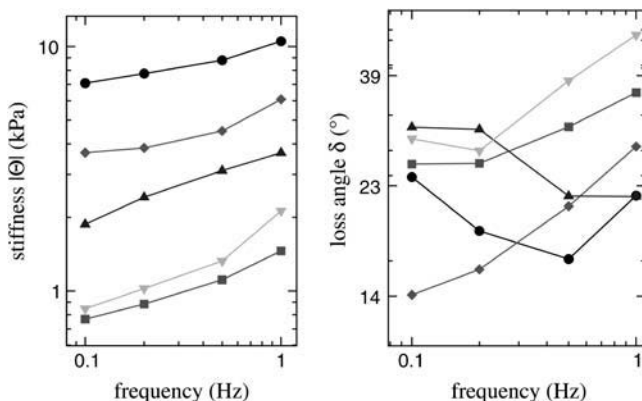


FIGURE 6 Frequency sweep (preliminary data). Modulus $|\Theta|$ and loss angle δ as a function of frequency. Each curve is obtained using a different cell.

A master relation characterizes stress stiffening

Not all fibroblasts generate such high forces as in the experiment shown in Fig. 3. To span a larger range of average force $\langle F \rangle$ and length $\langle \ell \rangle$, we step-stretch the cell and then keep the average length constant, superimposing oscillations to record the moduli Θ' and Θ'' . The procedure is periodically repeated, as shown in Fig. 8. As a reaction to a sudden change in length, a force relaxation always occurs, usually followed by active contraction. As the average force $\langle F \rangle$ evolves at a fixed length $\langle \ell \rangle$, the viscoelastic moduli are continuously recorded. We also perform step experiments controlling the average force $\langle F \rangle$. In this way, it is possible to span large areas in the $\langle \ell \rangle$ - $\langle F \rangle$ diagram.

We see that both viscoelastic moduli depend only on the average force, and are independent of the average length.

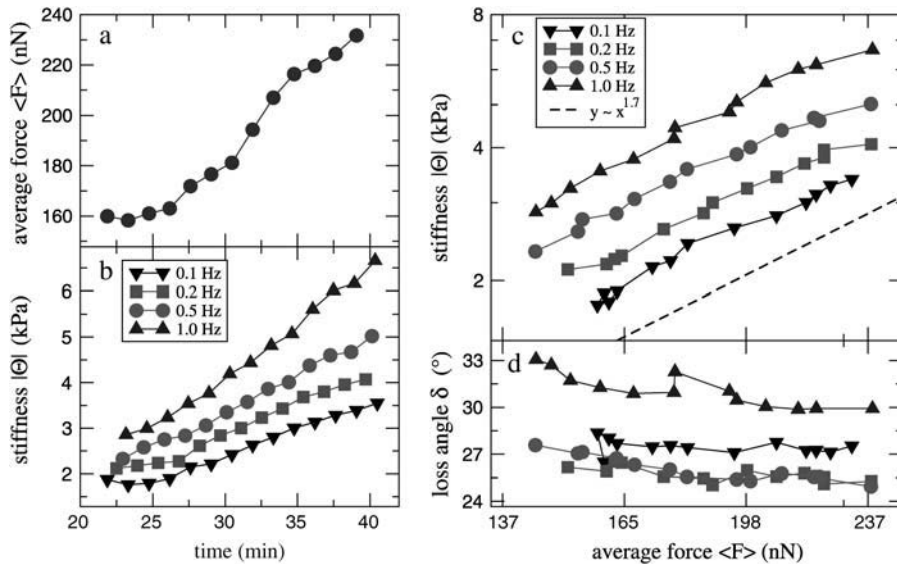


FIGURE 7 Stress stiffening due to active contraction at constant length. The average cell length is kept constant throughout at $\langle \ell \rangle = 9 \mu\text{m}$. Sinusoidal oscillations are superimposed with a strain amplitude $\Delta \ell / \langle \ell \rangle = 0.03$. The frequency of the oscillations is cyclically changed from 0.1 to 1.0 Hz. (a) The average force $\langle F \rangle$ is seen to increase in time. (b) The modulus $|\Theta|$ increases in time for all frequencies. (c) Stiffness $|\Theta|$ as a function of average force $\langle F \rangle$, for different frequencies. The line shows a power law function $y \sim x^{1.7}$ for comparison. (d) Loss angle δ as a function of average force $\langle F \rangle$, for different frequencies.

The dependence of the loss angle $\delta = \arctan(\Theta''/\Theta')$ on the average force $\langle F \rangle$ is erratic and weak, at most decreasing $\sim 20\%$ in the whole force range. As a function of the individual cell, it is within the range $10\text{--}30^\circ$. The absolute modulus $|\Theta| = (\Theta'^2 + \Theta''^2)^{1/2}$ remains constant at low forces, in a $1\text{--}30 \text{ kPa}$ range, depending on the individual cell. Above a cell-dependent crossover force, we observe stress stiffening: $|\Theta|$ increases as a function of the average force $\langle F \rangle$. This dependence of $|\Theta|$ on the average force can be well approximated by a power law, as shown in Fig. 9 (inset). More than one stress decade above crossover, most cells deform significantly and begin to detach or yield.

A collapse of all data to a single master relation can be achieved by introducing cell-dependent scaling factors, the zero force stiffness Θ_0 , and the crossover stress σ_C . On the average,

$$|\Theta| = \begin{cases} \Theta_0 & \text{for } \langle \sigma \rangle < \sigma_C \\ \Theta_0 \left(\frac{\langle \sigma \rangle}{\sigma_C} \right)^\gamma & \text{for } \langle \sigma \rangle > \sigma_C \end{cases}$$

The exponent γ is independent of the scaling factors. At 26°C , 0.2 Hz, and 5% deformation amplitude, it is ~ 1 , as shown by the collapsed data in Fig. 9. The scaling factors are roughly related by $\Theta_0 \propto \sigma_C^{1.3}$. Thus, an approximate collapse can be reached with a single parameter.

This master relation is consistently found in all cells strong enough to reach average stresses above $\sim 0.1 \Theta_0$. This reproducibility shows that oscillatory measurements are effective in probing cell mechanical properties independently of an underlying slow active behavior.

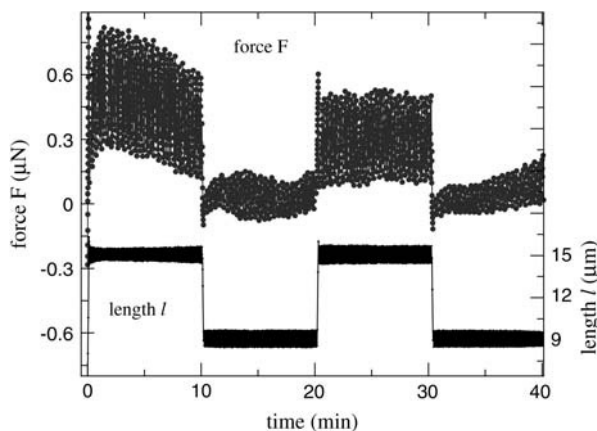


FIGURE 8 Force response as result of imposed length changes. We step-strain the cell by $\sim 50\%$ at a rate of $1.5 \mu\text{m/s}$, and apply length oscillations at an amplitude of $0.5 \mu\text{m}$ and a frequency of 0.2 Hz. The experiment was performed using fibronectin mediated adhesion.

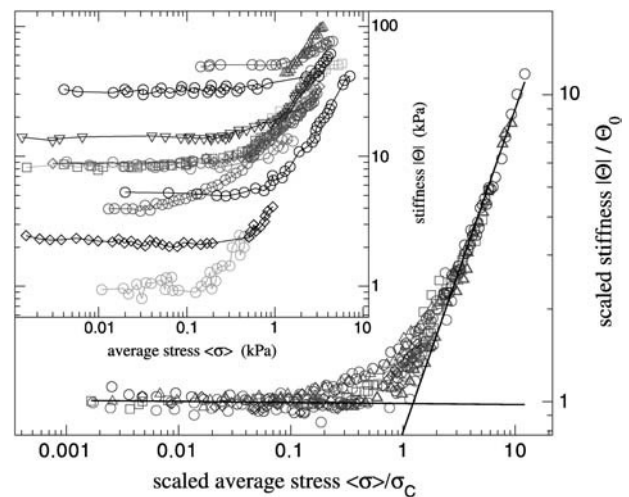


FIGURE 9 Inset shows the modulus $|\Theta|$ as a function of average stress for 13 cells, measured using length steps plus oscillation experiments such as in Fig. 8. The main plot shows the data scaled using two factors, as described in the text, which gives an exponent $\gamma \approx 1.0$. All experiments are performed at 26°C and using fibronectin mediated adhesion.

Ramp experiments with superimposed oscillations

The master relation holds at a constant cell length while an underlying active contraction occurs. In this case, the rate of change of the average stress is set by the cell. As a means of assessing the validity of the master relation while the average cell length changes, we increase $\langle \ell \rangle$ at a constant rate in the range 0.1–2 $\mu\text{m/s}$, and simultaneously superimpose small oscillations at an amplitude $\Delta \ell \simeq 0.5 \mu\text{m}$ and a frequency of 1 Hz, to measure the dynamic moduli Θ' and Θ'' . As shown in Fig. 10 *a*, by stretching the cell, a change in average stress is induced. The average stress $\langle \sigma \rangle$ depends roughly linearly on the average length $\langle \ell \rangle$ throughout a ramp. Remarkably, stress stiffening of the dynamic moduli is simultaneously observed. The master relation between $|\Theta|$ and $\langle \sigma \rangle$ is seen to remain valid at low deformation rates. These experiments show that the particular way of sweeping force space is not relevant, since the $|\Theta|(\langle \sigma \rangle)$ function is qualitatively the same as that found in active contraction experiments. Only at rates higher than a cell-dependent value in the vicinity of 100 nm/s,

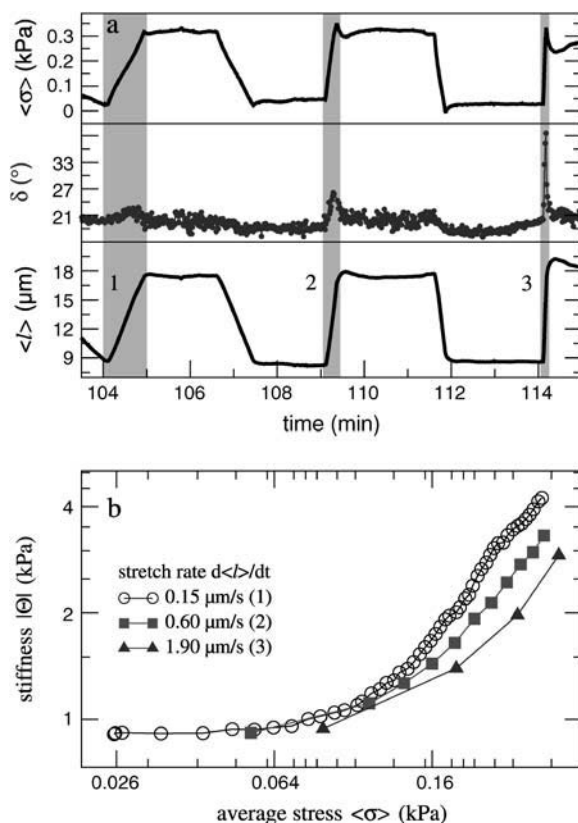


FIGURE 10 (a) Ramp experiment with glutaraldehyde coating. Average stress (top), loss angle (middle), and average length (bottom) as a function of time. Oscillations at 1 Hz, 5% amplitude are superposed throughout, also during the ramps (shaded areas). The loss angle δ increases with the deformation rate. (b) Stiffness as a function of average stress. The relationship between $|\Theta|$ and $\langle \sigma \rangle$ depends on the deformation rate. The curves correspond to the shaded areas 1, 2, and 3 in *a*.

$|\Theta|(\langle \sigma \rangle)$ falls below the master relation, and the cell becomes more fluid as evidenced by an increase in the loss angle δ (see Fig. 10, *a* and *b*). In general, the master relation cannot be deduced from the relationship between the average values $\langle \sigma \rangle$ and $\langle \ell \rangle$, since these are linearly related in a ramp experiment. This absence of stiffening agrees well with results from ramp experiments on whole tissues (1,16) and fibroblast-populated collagen gels (15).

Cytoskeleton perturbation using drugs

To distinguish between different cytoskeletal subcomponents, experiments are performed in presence of drugs, which disrupt specific filament types. Only cells able to sustain tensions above σ_C are subsequently treated with drugs. We observe sudden detachment of the cells from glutaraldehyde-coated microplates with the actin depolymerization inducer latrunculin A at 1 $\mu\text{g/ml}$ (27). The same effect is seen with the myosin heavy chain ATPase inhibitor 2,3-butanedione-monoxime at 2 mg/ml (28), as well as with the myosin light chain kinase inhibitor ML-7 at 100 μM (29). Since transmembrane proteins are covalently bound to the glutaraldehyde coating, they must rip off from the membrane during drug-induced cell detachment. Thus, the cell membrane alone is not able to hold transmembrane proteins under significant tension. An internal structure must bear the load under normal conditions. After disruption of either actin or myosin activity, this structure cannot sustain strong forces anymore. At fourfold lower concentrations, latrunculin A and ML-7 reduce $|\Theta|$ up to a factor of 5, whereas $\langle \sigma \rangle$ goes to zero. No significant effect is seen with the microtubule-disrupting drug nocodazole at 10 $\mu\text{g/ml}$ (30). Taken together, these results show that the actomyosin system bears the tension, without any other significant force-bearing structure in parallel.

Stress stiffening with glutaraldehyde coatings

To reduce active responses, we use glutaraldehyde-amino-silane coated walls, where accessible membrane proteins are covalently and nonspecifically bound through imine groups. Further, the serum concentration is reduced to 2%. In this way, the biochemical conditions are changed, but the experimental cell geometry remains the same. Active responses are indeed found to be weaker in these conditions. Compared to fibronectin-mediated adhesion, the stiffness values are scaled down by about a factor of three. However, the master relation between $|\Theta|$ and $\langle \sigma \rangle$ can still be observed.

DISCUSSION

The master relation is a general feature, which reproducibly occurs in our experiments. It holds during active contraction and adaptive responses, such as those seen in Figs. 3, 7, and 8, as well as in ramp experiments with superimposed oscillations, as in Fig. 10 *b*. It is observed in different biochemical

environments, which change the intensity of active responses. From this generality of the master relation, we conclude that it reflects a fundamental property of the cell force-bearing elements.

Stress stiffening in actin networks

Our cytoskeleton perturbation experiments point toward the actin network as the main component responsible for stress stiffening. Actin filaments, with a persistence length of 15 μm (5,31), behave as semiflexible filaments *in vivo*, where typical filament lengths are $\sim 1 \mu\text{m}$. It has recently become apparent that cross-linked as well as entangled networks of semiflexible filaments show characteristic nonlinear mechanical behavior. *In vitro* prestressed biopolymer gels under shear deformation, including cross-linked actin networks, generally show a transition from a linear regime to power law strain stiffening (6,7,32–34). The connection to our results has to be established with care. *In vitro* gels are passive minimal systems, generally studied under shear deformations. Instead, the living cell is a complex entity where a multitude of cross-linking proteins are available, many of them of a dynamic nature. Cytoskeletal restructuring might take place within an oscillation period. Keeping this in mind, we still find the qualitative similarity between the stiffness-force relations very suggestive. In scruiin cross-linked actin networks (7), the ratio between the crossover stress and the zero force modulus is of the order of 10^{-1} , and the stress-stiffening exponent is in the range 1–1.5, in remarkable agreement with our results. In experiments on filamin cross-linked actin gels (6), where the storage modulus G' is actually studied as a function of strain, the crossover strain is also of this order.

Intrinsic stress stiffening

The master relation connects the viscoelastic moduli to the average force independently of cell length. Rather than strain stiffening, fibroblasts exhibit intrinsic stress stiffening. To reconcile this to our interpretation of the master relation, we postulate that the internal strain of the gel, i.e., the stress, uncouples from the cell length ℓ as a result of active contraction, via rearrangements of the connection points of the network.

As shown by ramp experiments with superimposed oscillations, the master relation holds even during an externally imposed length increase, if the extension rate is sufficiently slow. The magnitude of the deformations that can then be imposed ($>50\%$), without the cell yielding, suggests that addition of material takes place. As the loss angle δ does not change under such conditions, we speculate that the cytoskeleton grows without major structural changes. The cytoskeleton is certainly capable of such restructuring, as exemplified by the growth under compression of the actin tail of *Listeria* (35,36), towed growth in neurites (37), or

stress fibers losing material while contracting (38). The maximal growth speed from our ramp experiments would be $\sim 6 \mu\text{m}/\text{min}$, in good agreement with the growth of the actin tails of the bacteria *Listeria* (35). At higher deformation rates, the cell starts to fluidize, which can be interpreted by an increased fraction of ruptured bonds.

Master relation in the context of cell mechanics

Several features of the master relation can be observed in experiments performed at very different length scales, corroborating our interpretation as a general feature of the force-bearing elements in the cell. This shows the master relation to be general, independent of the type of mechanical experiment or cell geometry. Uniaxial stretching experiments performed on skin, myosin fibers, tendons (1,16,17), and on fibroblast-populated collagen gels (15) show proportionality between dynamic stiffness and force. These results can be seen as a particular case of power law stress stiffening, for an exponent $\gamma = 1$.

Our results are also similar to stress stiffening in skeletal and smooth muscle, where stiffness is proportional to force. The generally accepted explanation is that both stiffness and force are a function of the variable number of actomyosin cross-bridges (39). Although such an explanation is attractive, it does not seem to apply to our case. We have measured forces up to 1 μN , in agreement with total forces exerted by spreading fibroblasts of $\sim 2 \mu\text{N}$ (2,40). This corresponds to $\sim 10^6$ myosins working in parallel, very close to the total amount reported in fibroblasts (41). Taking cross-bridge stiffness as 0.6 pN/nm (5), an arrangement of 10^6 myosins in parallel would be a factor of 100 stiffer than the maximum $|\Theta|$ we have measured in fibroblasts.

At the subcellular scale, microrheology experiments performed on adhering cells show proportionality between the shear storage modulus G' of the actin cortex and the force applied by the cell on the substrate (12). Here, the force was increased by stimulating cell contractility with histamine, or decreased by the relaxing agonist isoproterenol. The result compares well to our observation of stress stiffening at constant length, though no crossover to a linear regime is reported here. Recently, simultaneous increase of both the storage and loss shear moduli G' and G'' of the actin cortex after stretching epithelial cells has been observed (13). Accordingly, we see stress stiffening of both longitudinal moduli Θ' and Θ'' when stretching the cell in a ramp experiment with superimposed oscillations. Thus, the fact that the master relation holds regardless of the way force space is explored agrees with these microrheological studies taken together.

A similar example of length scale invariance is given by the agreement between microrheological studies in the frequency domain (14,25) and whole-cell experiments in the time domain (26). Fabry et al. (14,25), studying the shear moduli G' and G'' of the actin cortex as a function of

frequency, could collapse data from cells in different conditions onto master curves. The response in the frequency domain as revealed by these microrheological procedures was subsequently found to agree with the power law creep function of single cells (26). Hence, scale invariance and self-similarity may well be general properties of cell mechanics in the force, as well as in the time-frequency domain.

Possible stiffening mechanisms

Aiming at describing cross-linked biopolymer networks, theoretical frameworks have been developed recently. Networks are modeled as a two-dimensional random arrangement of filaments, characterized by a bending and a stretching modulus. Temperature effects have been addressed by including an entropic stretching modulus (8,42). At a nonzero temperature, thermal energy is stored in bending fluctuations, so that the distance between cross-links is smaller than the actual contour length of the filament. Separating these cross-links by stretching reduces the amplitude of these shape fluctuations, which gives rise to an increased effective stretching modulus. In general, the mechanical response of two-dimensional random networks depends strongly on the length scales involved, the filament length, and the mesh size ξ (the average distance between filaments). For long filament lengths or small mesh sizes, the deformation of the network is affine, i.e., the macroscopic mechanical response is essentially given by that of single filaments (8). The nonlinear elasticity of cross-linked biopolymer networks has been explained in terms of random networks (6,7), as an affine stretching-dominated regime where the macroscopic response is given by single-filament entropic stretching. This response is highly nonlinear, since thermal fluctuations are suppressed as the filament ends are separated close to full contour length. At high forces, the stiffness-force relation becomes a power law with exponent 3:2 (7).

An alternative explanation for stiffening in cross-linked random networks has been recently presented by Onck et al. (43). Here, stiffening arises as a transition from bending to stretching. Thermal effects are mostly irrelevant; increasing the temperature from 0 to 300 K increases the crossover strain, but does not affect the stiffening regime. Also, the transition to stiffening arises despite a certain degree of nonaffinity.

Below, we point out some remarkable features of single filament bending response that may be relevant for cross-linked filament networks. We discuss the bending response of inextensible filaments, characterized by a length L and a bending modulus κ . We show that bending itself shows a crossover to power law stress stiffening with an exponent 1.75, as well as a crossover strain of the order of 10^{-1} . This can be seen in Fig. 11. At large forces, the stiffness-force relation becomes a power law with exponent 3:2, similar to the entropic stretching response. The details of the calculation are left to the Appendix. It is noteworthy that many features of the master relation are similar to the mechanical

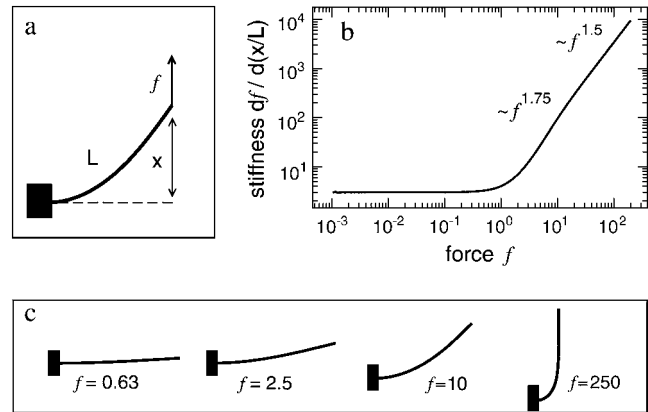


FIGURE 11 (a) Single-filament nonlinear elasticity: filaments are regarded as inextensible, characterized by a contour length L and a bending modulus κ . One end is clamped, the other one free. The force F bends the filament by an amount x . The dimensionless force is defined as $f = FL^2/\kappa$. (b) Differential stiffness $df/d(x/L)$ as a function of the dimensionless force f . (c) Euler-Bernoulli elastica: filament shapes for different forces.

response of single filaments. The experimental fact that a single parameter is sufficient to obtain the master relation may be captured by both the force and stiffness scales varying as κ/L^2 . Interestingly, the magnitude of the experimental crossover stress, when expressed as a strain σ_c/Θ_0 , is of the order of 10^{-1} , in good agreement with the theoretical crossover strain. As Fig. 11 *b* shows, the first force decade above crossover of the theoretical stiffness-force relation is an approximate power law with exponent 1.7, within the experimentally observed range. Further, the magnitude of the force scale is the right one if one assumes a realistic cytoskeleton mesh size of 100 nm (5,44,45) and an actin-bending modulus of $\kappa = 60 \text{ nN}(\text{nm})^2$ (5). This corresponds to the open-cell foam model proposed by Satcher and Dewey as a general model for the cytoskeleton (44), which gives a zero-force stiffness $\Theta_0 \sim 10 \text{ kPa}$, in good agreement with our measurements and with literature (17,44).

These observations suggest that the bending response of filaments may play a role in the nonlinear mechanical properties of cross-linked gels. Therefore, it is worthwhile considering this effect in further modeling of such systems. With these experiments, we cannot distinguish between the different mechanisms proposed for stiffening. Further experimental work and theoretical modeling will be required to elucidate the relative contributions of these effects for physiologically relevant values of mesh sizes and filament lengths.

SUMMARY, CONCLUSION, AND OUTLOOK

By performing single fibroblast mechanical measurements, we have revealed a master relation relating stress and dynamical cell stiffness. This relation is obtained by a simple scaling of data from different cells. For the measurement, we

use the fact that cells are active: as a reaction to a sudden perturbation, the cell sweeps a range of mechanical stresses. We probe the cell elastic properties during this active response. Despite this underlying complex behavior that may involve multiple biochemical pathways, the master relation is surprisingly simple and reproducible. If the average force is externally changed, by slowly stretching the cell in a ramp experiment while superimposing small-amplitude oscillations, the master relation between $\langle F \rangle$ and the stiffness $|\Theta|$ is seen again. Thus, a distinction between active and passive stress is artificial—regardless of deformation history, the response to small perturbations is always given by the average force. In view of this generality, and the remarkable agreement with the mechanic behavior of biopolymer networks, we interpret the master relation as revealing the nonlinear response of the actin network.

These experiments provide a framework where simplified biomimetic systems can be connected to living cell mechanics. Here, the active nature of the cytoskeleton is naturally integrated into the phenomenology. Along these lines, we are currently extending our frequency and amplitude range, to undertake a more detailed analysis of the master relation.

As a final remark, fibroblasts reach the stress-stiffening regime naturally by active contraction, and we expect the crossover force to be within the physiological force range. Thus, stress stiffening may play a role in vivo. For example, cells are known to sense the extracellular elasticity and exert forces along lines of maximum effective stiffness, a process that has been modeled within linearized elasticity (3). In the future, power law stress stiffening could be included in the modeling of cell organization by mechanosensing.

APPENDIX: BENDING RESPONSE OF AN INEXTENSIBLE FILAMENT

In what follows, we show that a transition to power law stiffening is already present in the nonlinearity of bending deformations. We analyze the mechanical response of inextensible filaments characterized by a bending modulus κ and a contour length L . We assume that the relationship between bending moment and curvature stays linear, so that any nonlinearity is of geometrical nature. The filament shape then corresponds to Euler-Bernoulli elastica (46). Our boundary conditions are one filament end free and the other one clamped perpendicular to the force direction, as illustrated in Fig. 11 *a*. These conditions are the minimum requirements for bending. At small strains x/L , the mechanical equilibrium equation can be linearized and the zero-force stiffness analytically calculated as $dF/dx = 3\kappa/L^3$.

Numerically solving the nonlinear equilibrium equation, we find a relatively sharp crossover to a strain-stiffening regime at strains $x/L > 0.3$, as shown in Fig. 11 *b*. At large strains, the stiffness-force relation asymptotically becomes a power law with an exponent 1.5. At high forces, the filament shape tends to a straight line along the force direction, with a sharp kink at the clamped end (see Fig. 11 *c*). In this limit, the effect of increasing F can be shown to be a scaling of the filament shape at the clamped end; the endpoint coordinates and curvature radius remain linearly related as they change as a function of F . Thus, we can introduce a force-dependent scaling factor ε , which tends to zero as the force is increased to infinity. In terms of this factor, the full contour length L and the projection length x (see Fig. 11 *a*) can be written as $L - x \propto \varepsilon$, and the torque balance equation as $F\varepsilon \propto 1/\varepsilon$. Therefore, $F \propto 1/(L - x)^2$, which gives power law stiffening, $dF/dx \propto F^{3/2}$.

In general, an entropic contribution to the longitudinal filament stretching modulus is expected due to thermal fluctuations. At low forces, this leads to a thermal longitudinal modulus $k_T = 90\kappa^2/(k_B T L^4)$ (42), where L is the contour length, and $k_B T$ the thermal energy. Taking a mesh size of 100 nm, this thermal longitudinal modulus k_T is about a factor of 10^4 larger than the low-force mechanical bending stiffness, $k_\perp = 3\kappa/L^3$. Since $k_\perp/k_T \propto L$, the mechanical response of a regular network such as the open-cell foam model (44) remains dominated by bending stiffness for physiological mesh sizes. Further, for such mesh sizes, the mechanical bending energy already exceeds the thermal energy at strains above $\sim 4\%$, well within the linear regime. Thus, thermal effects are not relevant for the bending response itself.

SUPPLEMENTARY MATERIAL

An online supplement to this article can be found by visiting BJ Online at <http://www.biophysj.org>.

We thank A. Bausch, G. Massiera, H. Brand, L. Mahadevan, O. Thoumine, F. Jülicher, and R. Everaers for helpful discussions, and B. Wehrle-Haller for his generous gift of GFP-actin fibroblasts. Assistance from A. Hanold in taking care of the cell culture is gratefully acknowledged. We also thank Y. Marcy and A. Micoulet for work on the setup. Finally, we are very grateful to the reviewers for constructive criticism and helpful suggestions, and to the editor for his interest in the manuscript.

This work has been funded by the Universität Bayreuth and the Institut Curie (Paris). Some of the results of this work were presented in the PHYNECS workshop in Peyresq, France, September 2002, and in the DPG Frühjahrstagung der Deutschen Physikalischen Gesellschaft, Regensburg, Germany, March 2004.

REFERENCES

1. Fung, Y. C. 1993. *Biomechanics: Mechanical Properties of Living Tissues*. Springer Verlag, New York.
2. Wrobel, L. K., T. R. Fray, J. E. Molloy, J. J. Adams, M. P. Armitage, and J. C. Sparrow. 2002. Contractility of single human dermal myofibroblasts and fibroblasts. *Cell Motil. Cytoskeleton*. 52:82–90.
3. Bischofs, I. B., and U. S. Schwarz. 2003. Cell organization in soft media due to active mechanosensing. *Proc. Natl. Acad. Sci. USA*. 100: 9274–9279.
4. Alberts, B., D. Bray, J. Lewis, M. Raff, K. Roberts, and J. Watson. 1994. *Molecular Biology of the Cell*, 3rd ed. Garland Publishing, New York.
5. Howard, J. 2001. *Mechanics of Motor Proteins and the Cytoskeleton*. Sinauer Associates, Sunderland, MA.
6. Storm, C., J. J. Pastore, F. C. MacKintosh, T. C. Lubensky, and P. A. Janmey. 2005. Nonlinear elasticity in biological gels. *Nature*. 435:191–194.
7. Gardel, M. L., J. H. Shin, F. C. MacKintosh, L. Mahadevan, P. Matsudaira, and D. A. Weitz. 2004. Elastic behavior of cross-linked and bundled actin networks. *Science*. 304:1301–1305.
8. Head, D. A., A. J. Levine, and F. C. MacKintosh. 2003. Deformation of cross-linked semiflexible polymer networks. *Phys. Rev. Lett.* 91:108102.
9. Humphrey, D., D. Duggan, D. Saha, D. Smith, and J. Käs. 2002. Active fluidization of polymer networks through molecular motors. *Nature*. 416:413–416.
10. Keller, M., R. Tharmann, M. A. Dichtl, A. R. Bausch, and E. Sackmann. 2003. Slow filament dynamics and viscoelasticity in entangled and active actin networks. *Philos. Trans. R. Soc. Lond. A*. 361:699–710.
11. Wang, N., J. P. Butler, and D. E. Ingber. 1993. Mechanotransduction across the cell surface and through the cytoskeleton. *Science*. 260:1124–1127.
12. Wang, N., I. M. Tolic-Nørrelykke, J. Chen, S. M. Mijailovich, J. P. Butler, J. J. Fredberg, and D. Stamenovic. 2002. Cell prestress. I.

- Stiffness and prestress are closely associated in adherent contractile cells. *Am. J. Physiol. Cell Physiol.* 282:C606–C616.
13. Trepatt, X., M. Grabulosa, F. Puig, G. N. Maksym, D. Navajas, and R. Farré. 2004. Viscoelasticity of human alveolar epithelial cells subjected to stretch. *Am. J. Physiol. Lung Cell. Mol. Physiol.* 287:L1025–L1034.
 14. Fabry, B., G. N. Maksym, J. P. Butler, M. Glogauer, D. Navajas, and J. J. Fredberg. 2001. Scaling the microrheology of living cells. *Phys. Rev. Lett.* 87:148102.
 15. Wakatsuki, T., M. S. Kolodney, G. I. Zahalak, and E. L. Elson. 2000. Cell mechanics studied by a reconstituted model tissue. *Biophys. J.* 79:2353–2368.
 16. Fung, Y. C. B. 1967. Elasticity of soft tissues in simple elongation. *Am. J. Physiol.* 213:1532–1544.
 17. Verdier, C. 2003. Rheological properties of living materials. From cells to tissues. *J. Theor. Med.* 5:67–91.
 18. Thoumine, O., and A. Ott. 1997. Time scale dependent viscoelastic and contractile regimes in fibroblasts probed by microplate manipulation. *J. Cell Sci.* 110:2109–2116.
 19. Todaro, G. J., and H. Green. 1963. Quantitative studies of the growth of mouse embryo cells in culture and their development into established lines. *J. Cell Biol.* 17:299–313.
 20. Todaro, G. J., K. Habel, and H. Green. 1965. Antigenic and cultural properties of cells doubly transformed by polyoma virus and sv40. *Virology.* 27:179–185.
 21. Drexler, H. G., W. Dirks, W. R. A. F. MacLeod, H. Quentmeier, K. G. Steube, and C. C. Uphoff. 2001. DSMZ Catalogue of Human and Animal Cell Lines. DSMZ, Braunschweig, Germany.
 22. Katsumi, A., A. Wayne Orr, E. Tzima, and M. A. Schwartz. 2004. Integrins in mechanotransduction. *J. Biol. Chem.* 279:12001–12004.
 23. Choquet, D., D. P. Felsenfeld, and M. P. Sheetz. 1997. Extracellular matrix rigidity causes strengthening of integrin-cytoskeleton linkages. *Cell.* 88:39–48.
 24. Findley, W. N., J. S. Lai, and K. Onaran. 1976. Creep and Relaxation of Nonlinear Viscoelastic Materials: With an Introduction to Linear Viscoelasticity. North-Holland Publishing, Toronto.
 25. Fabry, B., G. N. Maksym, J. P. Butler, M. Glogauer, D. Navajas, N. A. Taback, E. J. Millet, and J. J. Fredberg. 2003. Time scale and other invariants of integrative mechanical behavior in living cells. *Phys. Rev. E.* 68:041914.
 26. Desprat, N., A. Richert, J. Simeon, and A. Asnacios. 2005. Creep function of a single living cell. *Biophys. J.* 88:2224–2233.
 27. Spector, I., N. R. Shochet, Y. Kashman, and A. Groweiss. 1983. Latrunculins: novel marine toxins that disrupt microfilament organization in cultured cells. *Science.* 219:493–495.
 28. Herrmann, C., J. Wray, F. Travers, and T. Barman. 1992. Effect of 2,3-butanedione monoxime on myosin and myofibrillar ATPases. An example of an uncompetitive inhibitor. *Biochemistry.* 31:12227–12232.
 29. Saitoh, M., T. Ishikawa, S. Matsushima, M. Naka, and H. Hidaka. 1987. Selective inhibition of catalytic activity of smooth muscle myosin light chain kinase. *J. Biol. Chem.* 262:7796–7801.
 30. De Brabander, M., R. Van de Veire, R. Aerts, M. Borgers, and P. Janssen. 1976. The effects of methyl[5-(2-thienylcarbonyl)-1H-benzimidazol-2-yl]carbamate (R 17 934, NSC 238159), a new synthetic antitumoral drug interfering with microtubules, on mammalian cells cultured in vitro. *Cancer Res.* 36:905–916.
 31. Ott, A., M. Magnasco, A. Simon, and A. Libchaber. 1993. Measurement of the persistence length of polymerized actin using fluorescence microscopy. *Phys. Rev. E.* 48:R1642–R1645.
 32. Janmey, P. A., S. Hvidt, J. Lamb, and T. P. Stossel. 1990. Resemblance of actin-binding protein/actin gels to covalently crosslinked networks. *Nature.* 345:89–92.
 33. Xu, J., Y. Tseng, and D. Wirtz. 2000. Strain hardening of actin filament networks. Regulation by the dynamic cross-linking protein α -actinin. *J. Biol. Chem.* 275:35886–35892.
 34. Groot, R. D., A. Bot, and W. G. M. Agterof. 1996. Molecular theory of strain hardening of a polymer gel: application to gelatin. *J. Chem. Phys.* 104:9202–9219.
 35. Gerbal, F., V. Noireaux, C. Sykes, F. Jülicher, P. Chaikin, A. Ott, J. Prost, R. Golsteyn, E. Friederich, D. Louvard, V. Laurent, and M. Carlier. 1999. On the *Listeria* propulsion mechanism. *Pramana-J. Phys.* 53:155–170.
 36. Marcy, Y., J. Prost, M. F. Carlier, and C. Sykes. 2004. Forces generated during actin-based propulsion: a direct measurement by micromanipulation. *Proc. Natl. Acad. Sci. USA.* 101:5992–5997.
 37. Dennerli, T. J., P. Lamoureux, R. E. Buxbaum, and S. R. Heidemann. 1989. The cytomechanics of axonal elongation and retraction. *J. Cell Biol.* 109:3073–3083.
 38. Kolega, J., L. W. Janson, and D. Lansing Taylor. 1991. The role of solation-contraction coupling in regulating stress fiber dynamics in nonmuscle cells. *J. Cell Biol.* 114:993–1003.
 39. Ford, L. E., A. F. Huxley, and R. M. Simmons. 1981. The relation between stiffness and filament overlap in stimulated frog muscle fibres. *J. Physiol.* 311:219–249.
 40. Dembo, M., and Y. L. Wang. 1999. Stresses at the cell-to-substrate interface during locomotion of fibroblasts. *Biophys. J.* 76:2307–2316.
 41. Bray, D., and C. Thomas. 1975. The actin content of fibroblasts. *Biochem. J.* 147:221–228.
 42. MacKintosh, F. C., J. Käs, and P. A. Janmey. 1995. Elasticity of semiflexible biopolymer networks. *Phys. Rev. Lett.* 75:4425–4428.
 43. Onck, P., T. Koeman, T. van Dillen, and E. van der Giessen. 2005. Alternative explanation of stiffening in cross-linked semiflexible networks. *Phys. Rev. Lett.* 95:178102.
 44. Satcher, R. L., and C. F. Dewey, Jr. 1996. Theoretical estimates of mechanical properties of the endothelial cell cytoskeleton. *Biophys. J.* 71:109–118.
 45. Medalia, O., I. Weber, A. S. Frangakis, D. Nicastro, G. Gerisch, and W. Baumeister. 2002. Macromolecular architecture in eucaryotic cells visualized by cryoelectron tomography. *Science.* 298:1209–1213.
 46. Love, A. E. H. 1944. A treatise on the mathematical theory of elasticity. Dover, New York.